

Filtering and Smoothing with Score-Driven Models*

Giuseppe Buccheri¹, Giacomo Bormetti², Fulvio Corsi^{3,4}, and Fabrizio Lillo^{2,5}

¹Scuola Normale Superiore, Italy

²University of Bologna, Italy

³University of Pisa, Italy

⁴City University of London, UK

⁵CADS, Human Technopole, Milan, Italy

Abstract

We propose a methodology for filtering, smoothing and assessing parameter and filtering uncertainty in misspecified score-driven models. Our technique is based on a general representation of the well-known Kalman filter and smoother recursions for linear Gaussian models in terms of the score of the conditional log-likelihood. We prove that, when data are generated by a nonlinear non-Gaussian state-space model, the proposed methodology results from a first-order expansion of the true observation density around the optimal filter. The error made by such approximation is assessed analytically. As shown in extensive Monte Carlo analyses, our methodology performs very similarly to exact simulation-based methods, while remaining computationally extremely simple. We illustrate empirically the advantages in employing score-driven models as misspecified filters rather than purely predictive processes.

Keywords: State-Space models, Score-driven models, Kalman filter, Smoothing, Filtering uncertainty

JEL codes: C22, C32, C58.

*Corresponding author: Giuseppe Buccheri, Scuola Normale Superiore, Piazza dei Cavalieri 7, 56126, Pisa (Italy). We are particularly grateful for suggestions we have received from Andrew Harvey, Marcin Zamojski and participants to the 11th CFE conference in London, the 11th SoFiE conference in Lugano, the 2018 IAAE conference in Montreal, the 2019 workshop on score-driven time-series models in Cambridge and the 2019 IAAE conference in Cyprus.

1 Introduction

GARCH-type models (Engle 1982, Bollerslev 1986) and, more generally, observation-driven models (Cox 1981), are a class of dynamic econometric models where the time-varying parameters depend on past observations. When these models are regarded as data generating processes, the time-varying parameters are completely revealed by past observations, which encode all the relevant information. As such, there is no room for smoothing and the only form of uncertainty is that coming from the finite sample distribution of the maximum likelihood estimates, called parameter uncertainty. On the other hand, observation-driven models can be regarded as predictive filters, since the time-varying parameters are one-step-ahead predictable. In this case, conditionally on past observations, the state variables have a non-degenerate density, called filtering uncertainty. This means that exploiting information from contemporaneous and future observations would provide better estimates compared to one-step-ahead predictions. Such idea was largely exploited by D. B. Nelson, who explored the properties of the conditional covariances of misspecified GARCH filters under the assumption that data are generated by a continuous-time diffusion¹; see Nelson (1992), Nelson and Foster (1994), Nelson and Foster (1995) and Nelson (1996). In particular, Nelson (1996) showed how to efficiently use information in both lagged and led GARCH residuals to estimate the spot volatility of a Brownian diffusion. Despite the considerable amount of observation-driven models proposed in the econometric literature, little attention has been paid to examine their properties as misspecified filters and, as a consequence, to use them for smoothing and for assessing filtering uncertainty.

We aim at filling this gap by introducing a filtering and smoothing methodology for a large subset of observation-driven models, namely the class of score-driven models of Creal et al. (2013) and Harvey (2013), also known as “Generalized Autoregressive Score” (GAS) models or “Dynamic Conditional Score” (DCS) models. Score-driven models have successfully been applied in the recent econometric literature; see for instance Creal et al. (2011), Harvey and Luati (2014), Oh and Patton (2017), Babii et al. (2019). We first show that the well-known Kalman filter and smoother recursions for linear Gaussian models can be written in terms of the score and a measure of curvature of the conditional log-likelihood function. In particular, the predictive filter has the form of a standard score-driven recursion, with a score normalization given by the conditional covariance of

¹The interpretation of GARCH processes as predictive filters is well described in this statement by Nelson (1992): “Note that our use of the term ‘estimate’ corresponds to its use in the filtering literature rather than the statistics literature; that is, an ARCH model with (given) fixed parameters produces ‘estimates’ of the true underlying conditional covariance matrix at each point in time in the same sense that a Kalman filter produces ‘estimates’ of unobserved state variables in a linear system”.

the underlying state variables. Motivated by such result, we extend the Kalman filter and smoother recursions written in terms of the score to a nonlinear non-Gaussian conditional density, obtaining a general methodology for score-driven filtering and smoothing in nonlinear non-Gaussian models. The formal equivalence between the Kalman predictive filter and score-driven models allows, on the one side, to provide a further justification for the updating rule adopted in score-driven models, and, on the other, to extend the additional tools available for linear Gaussian models to misspecified score-driven models, namely: (i) the update filter, (ii) the smoother and (iii) the computation of confidence bands accounting for both parameter and filtering uncertainty.

The problem of filtering and smoothing for general state-space models reduces to a multi-dimensional integral over the space spanned by the state-variables. Simulation-based techniques are typically employed to compute such integrals (see e.g. Durbin and Koopman 2012). If one assumes that data are generated by a nonlinear non-Gaussian state-space model, it is natural asking what kind of approximation one makes by replacing the optimal but computationally intense filter with the score-driven filter. We show that, under a specific normalization, score-driven filters result from a first-order expansion of the true observation density in a neighbourhood of the optimal filter of the underlying state-space model. Such result allows us to assess analytically the approximation error, which turns out to be related to filtering uncertainty, and to contrast score-driven filters to other approximate filtering algorithms based on different approximations.

The main advantage of the proposed methodology is that its computational complexity is the same as in linear Gaussian models. The predictive and update filters are indeed computed iteratively through a simple forward recursion. Smoothing only requires an additional backward recursion, which updates the filtered estimates using the information of all the available data. The second conditional moments follow similar recursions. Even the estimation of the static parameters simplifies considerably, since we recover an approximate closed-form formula for the log-likelihood function. Despite its computational simplicity, the methodology provides very close results to exact simulation-based methods. This is confirmed by our simulation study, which compares score-driven filtered and smoothed estimates with those obtained from exact methods.

As evidenced above, correctly specified observation-driven models are only affected by parameter uncertainty, which comes from replacing the true static parameters with their maximum likelihood estimates. However, if observation-driven models are employed as misspecified filters, the latent state variables are not completely revealed by past observations. Thus, also filtering uncertainty is relevant when building confidence bands. While parameter uncertainty can be quantified through the methods developed e.g. by Pascual et al. (2006) and Blasques et al. (2016), it is less clear how one can take into account filtering uncertainty in observation-driven models. By employing

the approximate conditional second moments provided by our recursions, we construct in-sample and out-of-sample confidence bands, in a similar fashion to linear Gaussian models. Furthermore, depending on the needs of the user, the constructed confidence bands can account for filtering uncertainty only, for parameter uncertainty only, or for both parameter and filtering uncertainty.

Beside the papers of D. B. Nelson mentioned above, observation-driven models have been employed as misspecified filters in other works. It is worth mentioning the paper of Blasques et al. (2015), who proved that score-driven filters are locally optimal based on information theoretic criteria, and that of Koopman et al. (2016), who showed through an extensive Monte Carlo study that misspecified score-driven models provide similar forecasting performances as correctly specified parameter-driven models. Harvey (2013) proposed a related smoothing technique for a dynamic Student- t location model by replacing the prediction error in the Kalman smoother recursions with the score of the Student- t density. An application of such technique can be found in Caivano et al. (2016). Our approach is based on a representation of the Kalman filter and smoother recursions in terms of the score of the conditional log-likelihood which leads to different smoothing recursions. The latter are readily applicable to a general nonlinear non-Gaussian density. We also discuss in detail how our method relates to other approximate filtering algorithms, like the popular algorithm of Masreliez (1975) and the approximation via mode estimation of Durbin and Koopman (2012).

By performing an extensive Monte Carlo study with different kinds of non-linear non-Gaussian state-space models, we compare the proposed methodology to exact simulation based methods. We find that the losses incurred by our approximate filtering and smoothing technique are very small in all the simulated scenarios, and are always lower, on average, than 2.5% in mean-square errors. Not surprisingly, computational times are much lower compared to exact methods. As a matter of fact, in our simulation study we find that the computational time of the score-driven algorithm is between 150 and 800 times smaller than that of importance sampling based methods. For the same set of nonlinear non-Gaussian models, we construct confidence bands around filtered and smoothed estimates, and find a substantial agreement between the average coverage rate and the nominal confidence level. The results also indicate that neglecting filtering uncertainty heavily underestimates the total uncertainty and leads to narrow confidence bands.

Our empirical study is devoted to show the advantages of employing score-driven models as misspecified filters rather than purely predictive processes. Using data of stocks belonging to the US equity market, we show that smoothing significantly improves over standard score-driven estimates, and that neglecting filtering uncertainty leads to a number of exceedances larger than expected when constructing confidence bands. We test the results using both univariate and multivariate stochastic volatility models. This is straightforward in our methodology, as it remains computationally simple

even at large dimensions.

The rest of the paper is organized as follows: Section (2) introduces the methodology, provides the main theoretical results and discusses the relation with other approximate filtering methods; Section (3) shows the results of the Monte Carlo study; in Section (4) the methodology is applied to a dataset of assets prices belonging to the Russel 3000 index; Section (5) concludes.

2 Methodology

2.1 Linear Gaussian models

Our starting point is the well-known theory of linear-Gaussian models. Let us consider the following state-space representation:

$$\mathbf{y}_t = \mathbf{Z}\boldsymbol{\alpha}_t + \boldsymbol{\epsilon}_t, \quad \boldsymbol{\epsilon}_t \sim \text{NID}(\mathbf{0}, \mathbf{H}) \quad (2.1.1)$$

$$\boldsymbol{\alpha}_{t+1} = \mathbf{c} + \mathbf{T}\boldsymbol{\alpha}_t + \boldsymbol{\eta}_t, \quad \boldsymbol{\eta}_t \sim \text{NID}(\mathbf{0}, \mathbf{Q}) \quad (2.1.2)$$

where $\boldsymbol{\alpha}_t \in \mathbb{R}^m$ is a vector of state variables and $\mathbf{y}_t \in \mathbb{R}^p$ is a vector of observations. The parameters $\mathbf{Z} \in \mathbb{R}^{p \times m}$, $\mathbf{H} \in \mathbb{R}^{p \times p}$, $\mathbf{T} \in \mathbb{R}^{m \times m}$ and $\mathbf{Q} \in \mathbb{R}^{m \times m}$ are referred to as system matrices. Let \mathbf{Y}_t denote the set of observations up to time t , namely $\mathbf{Y}_t = \{\mathbf{y}_1, \dots, \mathbf{y}_t\}$. We are interested in computing the mean and the variance of the underlying state variable $\boldsymbol{\alpha}_t$ based on the observations $\mathbf{y}_1, \dots, \mathbf{y}_t$ available at time t (update step) and in computing the mean and the variance of $\boldsymbol{\alpha}_{t+1}$ based on the past observations $\mathbf{y}_1, \dots, \mathbf{y}_t$ (prediction step). We thus define:

$$\mathbf{a}_{t|t} = \mathbb{E}[\boldsymbol{\alpha}_t | \mathbf{Y}_t], \quad \mathbf{P}_{t|t} = \mathbb{V}[\boldsymbol{\alpha}_t | \mathbf{Y}_t] \quad (2.1.3)$$

$$\mathbf{a}_{t+1} = \mathbb{E}[\boldsymbol{\alpha}_{t+1} | \mathbf{Y}_t], \quad \mathbf{P}_{t+1} = \mathbb{V}[\boldsymbol{\alpha}_{t+1} | \mathbf{Y}_t] \quad (2.1.4)$$

The Kalman filter allows to compute recursively $\mathbf{a}_{t|t}$, $\mathbf{P}_{t|t}$, \mathbf{a}_{t+1} and \mathbf{P}_{t+1} . Assuming $\boldsymbol{\alpha}_1 \sim \text{N}(\mathbf{a}_1, \mathbf{P}_1)$, where \mathbf{a}_1 and \mathbf{P}_1 are known, for $t = 1, \dots, n$, we have (see e.g. Harvey 1991, Durbin and Koopman 2012):

$$\mathbf{v}_t = \mathbf{y}_t - \mathbf{Z}\mathbf{a}_t \quad (2.1.5)$$

$$\mathbf{a}_{t|t} = \mathbf{a}_t + \mathbf{P}_t \mathbf{Z}' \mathbf{F}_t^{-1} \mathbf{v}_t \quad (2.1.6)$$

$$\mathbf{a}_{t+1} = \mathbf{c} + \mathbf{T}\mathbf{a}_t + \mathbf{K}_t \mathbf{v}_t \quad (2.1.7)$$

and:

$$\mathbf{F}_t = \mathbf{Z}\mathbf{P}_t\mathbf{Z}' + \mathbf{H} \quad (2.1.8)$$

$$\mathbf{P}_{t|t} = \mathbf{P}_t - \mathbf{P}_t \mathbf{Z}' \mathbf{F}_t^{-1} \mathbf{Z}\mathbf{P}_t \quad (2.1.9)$$

$$\mathbf{P}_{t+1} = \mathbf{T}\mathbf{P}_t(\mathbf{T} - \mathbf{K}_t\mathbf{Z}') + \mathbf{Q} \quad (2.1.10)$$

where $\mathbf{K}_t = \mathbf{TP}_t\mathbf{Z}'\mathbf{F}_t^{-1}$. The conditional log-likelihood is normal and is given by:

$$\log p(\mathbf{y}_t|\mathbf{Y}_{t-1}) = \text{const} - \frac{1}{2} (\log |\mathbf{F}_t| + \mathbf{v}_t'\mathbf{F}_t^{-1}\mathbf{v}_t) \quad (2.1.11)$$

The smoothed estimates $\hat{\boldsymbol{\alpha}}_t = \mathbb{E}[\boldsymbol{\alpha}_t|Y_n]$, $\hat{\mathbf{P}}_t = \mathbb{V}[\boldsymbol{\alpha}_t|Y_n]$, $n > t$, can instead be computed through the following set of backward recursions:

$$\mathbf{r}_{t-1} = \mathbf{Z}'\mathbf{F}_t^{-1}\mathbf{v}_t + \mathbf{L}_t'\mathbf{r}_t \quad (2.1.12)$$

$$\hat{\boldsymbol{\alpha}}_t = \mathbf{a}_t + \mathbf{P}_t\mathbf{r}_{t-1} \quad (2.1.13)$$

and:

$$\mathbf{N}_{t-1} = \mathbf{Z}'\mathbf{F}_t^{-1}\mathbf{Z} + \mathbf{L}_t'\mathbf{N}_t\mathbf{L}_t \quad (2.1.14)$$

$$\hat{\mathbf{P}}_t = \mathbf{P}_t - \mathbf{P}_t\mathbf{N}_{t-1}\mathbf{P}_t \quad (2.1.15)$$

where $\mathbf{L}_t = \mathbf{T} - \mathbf{K}_t\mathbf{Z}$, $\mathbf{r}_n = \mathbf{0}$, $\mathbf{N}_n = \hat{\mathbf{0}}$ and $t = n, \dots, 1$. The conditional distribution of $\boldsymbol{\alpha}_t$ is Gaussian with mean and variance given by $(\mathbf{a}_{t+1}, \mathbf{P}_{t+1})$, $(\mathbf{a}_{t|t}, \mathbf{P}_{t|t})$, $(\hat{\boldsymbol{\alpha}}_t, \hat{\mathbf{P}}_t)$, depending on the conditioning set.

2.2 Score-driven filtering and smoothing

Let us denote by $\boldsymbol{\nabla}_t = \frac{\partial \log p(\mathbf{y}_t|\mathbf{Y}_{t-1})}{\partial \mathbf{a}_t}$ the score of the conditional log-likelihood computed with respect to the predictive filter \mathbf{a}_t . From Eq. (2.1.11), it readily follows that in linear Gaussian models the score $\boldsymbol{\nabla}_t$ is given by:

$$\boldsymbol{\nabla}_t = \mathbf{Z}'\mathbf{F}_t^{-1}\mathbf{v}_t \quad (2.2.1)$$

Let also denote by $\boldsymbol{\mathcal{H}}_t$ the Hessian of the conditional log-likelihood function $p(\mathbf{y}_t|\mathbf{Y}_{t-1})$, defined as the matrix of second partial derivatives with respect to \mathbf{a}_t , namely:

$$\boldsymbol{\mathcal{H}}_t^{(hk)} = \frac{\partial^2 \log p(\mathbf{y}_t|\mathbf{Y}_{t-1})}{\partial \mathbf{a}_t^{(h)} \partial \mathbf{a}_t^{(k)}} \quad (2.2.2)$$

In linear Gaussian models we have:

$$\boldsymbol{\mathcal{H}}_t = -\mathbf{Z}'\mathbf{F}_t^{-1}\mathbf{Z} \quad (2.2.3)$$

It is immediate to re-write the Kalman filter and smoother equations in terms of $\boldsymbol{\nabla}_t$ and $\boldsymbol{\mathcal{H}}_t$. Indeed, Eq. (2.1.6), (2.1.7) become:

$$\mathbf{a}_{t|t} = \mathbf{a}_t + \mathbf{P}_t\boldsymbol{\nabla}_t \quad (2.2.4)$$

$$\mathbf{a}_{t+1} = \mathbf{c} + \mathbf{Ta}_t + \mathbf{TP}_t\boldsymbol{\nabla}_t \quad (2.2.5)$$

whereas Eq. (2.1.9), (2.1.10) become:

$$\mathbf{P}_{t|t} = \mathbf{P}_t + \mathbf{P}_t \mathbf{H}_t \mathbf{P}_t \quad (2.2.6)$$

$$\mathbf{P}_{t+1} = \mathbf{T} \mathbf{P}_t (\mathbf{T} + \mathbf{T} \mathbf{P}_t \mathbf{H}_t)' + \mathbf{Q} \quad (2.2.7)$$

Similarly, the backward smoothing recursions (2.1.12)-(2.1.15) can be written as:

$$\mathbf{r}_{t-1} = \nabla_t + \mathbf{T}(\mathbb{I} + \mathbf{P}_t \mathbf{H}_t) \quad (2.2.8)$$

$$\hat{\boldsymbol{\alpha}}_t = \mathbf{a}_t + \mathbf{P}_t \mathbf{r}_{t-1} \quad (2.2.9)$$

and:

$$\mathbf{N}_{t-1} = -\mathbf{H}_t + (\mathbb{I} + \mathbf{P}_t \mathbf{H}_t)' \mathbf{T}' \mathbf{H}_t \mathbf{T} (\mathbb{I} + \mathbf{P}_t \mathbf{H}_t) \quad (2.2.10)$$

$$\hat{\mathbf{P}}_t = \mathbf{P}_t - \mathbf{P}_t \mathbf{N}_{t-1} \mathbf{P}_t \quad (2.2.11)$$

The above representation is equivalent to the one in Section (2.1), but has a more general structure, as it can be applied given an arbitrary, twice differentiable non-Gaussian conditional density $p(\mathbf{y}_t | \mathbf{Y}_{t-1})$. The main idea of our methodology is to approximate the first and second conditional moments of the underlying state variables with the above recursions. In other words, given a nonlinear state-space model characterized by a non-Gaussian observation density $p(\mathbf{y}_t | \boldsymbol{\alpha}_t)$, we use Eq. (2.2.4)-(2.2.11) for filtering, smoothing and for computing the conditional covariance. In Section (2.3), we discuss the relation between the conditional density $p(\mathbf{y}_t | \mathbf{Y}_{t-1})$ used in the approximate recursions and the true observation density $p(\mathbf{y}_t | \boldsymbol{\alpha}_t)$. In particular, we show that applying our methodology is equivalent to performing a first-order Taylor expansion of $p(\mathbf{y}_t | \boldsymbol{\alpha}_t)$ in the neighbourhood of the optimal filter of the underlying state-space model. This allows us to characterize analytically the error made by replacing the optimal with the approximate filter.

As discussed in Section (2.4), the predictive filter in Eq. (2.2.5) belongs to the class of score-driven models of Creal et al. (2013) and Harvey (2013). In these models, the time-varying parameters are driven by the score ∇_t of the conditional log-likelihood function. Thus, the above recursions provide a further justification, in addition to the result of Blasques et al. (2015), for the update rule adopted in score-driven models. Compared to standard score-driven models, where the score is normalized by an arbitrary matrix \mathbf{S}_t , the above algorithm selects a specific normalization, the one given by Eq. (2.2.7). Under such normalization, Eq. (2.2.4)-(2.2.11) provide a methodology for filtering and smoothing in misspecified score-driven models. Similarly, the results of Section (2.3) characterize the properties of such models when employed as misspecified filters for nonlinear non-Gaussian models.

We finally observe that, in linear Gaussian models, the conditional Fisher information matrix $\mathbf{I}_t = \mathbb{E}[\nabla_t \nabla_t' | \mathbf{Y}_{t-1}] = \mathbf{Z}' \mathbf{F}_t^{-1} \mathbf{Z}$ is equal to the negative Hessian. Thus, we can also express Eq. (2.2.4)-(2.2.11) in terms of \mathbf{I}_t rather than \mathcal{H}_t . However, in nonlinear non-Gaussian models, the previous relation only holds in expectation, namely $\mathbf{I}_t = -\mathbb{E}[\mathcal{H}_t | \mathbf{Y}_{t-1}]$. Thus, to keep our formulation general, we express the recursions in terms of \mathcal{H}_t rather than \mathbf{I}_t .

2.3 Statistical properties

In this section we examine in more detail the nature of the approximation made by the filtering algorithm proposed in Section (2.2). For simplicity, we restrict our attention to univariate models. Let us consider the following nonlinear non-Gaussian state-space model:

$$y_t | \alpha_t \sim p(y_t | \alpha_t) \quad (2.3.1)$$

$$\alpha_{t+1} = c + \phi \alpha_t + \eta_t \quad (2.3.2)$$

where η_t has zero mean and variance q . We do not require η_t being normal. As in linear-Gaussian models, we denote by $a_{t|t} = \mathbb{E}[\alpha_t | \mathcal{F}_t]$, $a_t = \mathbb{E}[\alpha_t | \mathcal{F}_{t-1}]$ the update and predictive filters and by $p_{t|t} = \mathbb{V}[\alpha_t | \mathcal{F}_t]$, $p_t = \mathbb{V}[\alpha_t | \mathcal{F}_{t-1}]$ the conditional variances. Hereafter, $p(y_t | \alpha_t)$ is considered as a function of α_t , whereas the observations y_1, \dots, y_t are regarded as being fixed. The following result holds:

Proposition 1. *Let $p(y_t | \alpha_t) \in C^2(\mathbb{R})$. Then:*

$$a_{t|t} = a_t + p_t \nabla_{t,a_t} + \mathcal{O}(p_t) \quad (2.3.3)$$

where

$$\nabla_{t,a_t} = \left. \frac{\partial \log p(y_t | \alpha_t)}{\partial \alpha_t} \right|_{a_t} \quad (2.3.4)$$

denotes the score of the observation density $p(y_t | \alpha_t)$ evaluated at a_t .

As shown in Appendix A, to prove Prop. 1, we expand at first-order the observation density $p(y_t | \alpha_t)$ in a neighbourhood of a_t and then compute the integral over the posterior density $p(\alpha_t | Y_t)$. The above result tells us that, if we replace the optimal update filter $a_{t|t}$ with $a_t + p_t \nabla_{t,a_t}$, the approximation error is of order p_t . In Appendix B, using the same approximation, we prove the following result:

Proposition 2. *Let $p(y_t | \alpha_t) \in C^2(\mathbb{R})$ and assume that $p(\alpha_t | Y_{t-1})$ is an even function of α_t . Then:*

$$p_{t|t} = p_t (1 - p_t \nabla_{t,a_t}^2) + \mathcal{O}(p_t^2) \quad (2.3.5)$$

where ∇_{t,a_t} is defined as in Prop. 1.

The interpretation of the result in Prop. 2 is similar to that in Prop. 1. Replacing the optimal conditional variance $p_{t|t}$ with $p_t(1 - p_t \nabla_{t,a_t}^2)$ leads to an error of order p_t^2 . The assumption that $p(\alpha_t|Y_{t-1})$ is an even function can be relaxed at the expense of including a skewness term in Eq. (2.3.5). It is immediate to prove the following corollary:

Corollary 1. *Under the assumptions of Prop. 1 and 2, we have:*

$$a_{t+1} = c + \phi a_t + \phi p_t \nabla_{t,a_t} + \mathcal{O}(p_t) \quad (2.3.6)$$

$$p_{t+1} = \phi^2 p_t (1 - p_t \nabla_{t,a_t}^2) + q + \mathcal{O}(p_t^2) \quad (2.3.7)$$

The above results can be used to construct an iterative filtering algorithm for the nonlinear non-Gaussian model described by Eq. (2.3.1), (2.3.2). Indeed, if one ignores the approximation error, Eq. (2.3.3)-(2.3.7) allow to compute recursively the approximate conditional mean and variance of α_t . In other words, at time t , one can recover the update and predictive filter as follows:

$$\hat{a}_{t|t} = \hat{a}_t + \hat{p}_t \nabla_{t,\hat{a}_t} \quad (2.3.8)$$

$$\hat{p}_{t|t} = \hat{p}_t (1 - \hat{p}_t \nabla_{t,\hat{a}_t}^2) \quad (2.3.9)$$

and

$$\hat{a}_{t+1} = c + \phi \hat{a}_t + \phi \hat{p}_t \nabla_{t,\hat{a}_t} \quad (2.3.10)$$

$$\hat{p}_{t+1} = \phi^2 \hat{p}_t (1 - \hat{p}_t \nabla_{t,\hat{a}_t}^2) + q \quad (2.3.11)$$

The true and the approximate conditional moments differ not only by the error induced by the Taylor expansion, but also because we replace on the right-hand side of Eq. (2.3.3)-(2.3.7) the true moments a_t and p_t with the approximate moments \hat{a}_t , \hat{p}_t computed through Eq. (2.3.10), (2.3.11). It is therefore interesting to characterize the additional error made by replacing a_t and p_t with \hat{a}_t and \hat{p}_t in Eq. (2.3.3)-(2.3.7). This can be done in the case where a_1 and p_1 are known. In Appendix D we show that the following result holds:

Proposition 3. *Let $p(y_t|\alpha_t) \in C^3(\mathbb{R})$ and assume that $p(\alpha_t|Y_{t-1})$ is an even function of α_t . Assume also that a_1, p_1 are known. Then:*

$$a_{t|t} = \hat{a}_t + \hat{p}_t \nabla_{t,\hat{a}_t} + \mathcal{O}(\hat{p}_t) \quad (2.3.12)$$

$$p_{t|t} = \hat{p}_t (1 - \hat{p}_t \nabla_{t,\hat{a}_t}^2) + \mathcal{O}(\hat{p}_t^2) \quad (2.3.13)$$

and

$$a_{t+1} = c + \phi \hat{a}_t + \phi \hat{p}_t \nabla_{t,\hat{a}_t} + \mathcal{O}(\hat{p}_t) \quad (2.3.14)$$

$$p_{t+1} = \phi^2 \hat{p}_t (1 - \hat{p}_t \nabla_{t,\hat{a}_t}^2) + q + \mathcal{O}(\hat{p}_t^2) \quad (2.3.15)$$

where $\hat{a}_1 = a_1$, $\hat{p}_1 = p_1$ and \hat{a}_t, \hat{p}_t are computed iteratively by Eq. (2.3.10), (2.3.11).

Prop. 3 quantifies the deviation of the approximate conditional moments in Eq. (2.3.8)-(2.3.11) from the true conditional moments. It states that, provided that we know a_1 and p_1 , the approximation error due to replacing a_t and p_t with \hat{a}_t and \hat{p}_t is of the same order as the one we would make if a_t and p_t were known.

Under the constraint that $p(y_t|Y_{t-1}) = p(y_t|\alpha_t)|_{\hat{a}_t}$, such algorithm is essentially equivalent to that described in Section (2.2). The only difference is due to the presence of the squared score in place of the negative Hessian in the equations for the conditional variance. Although the two quantities are equal in expectation, they differ by the term $\frac{1}{p(y_t|\alpha_t)} \frac{\partial^2 p(y_t|\alpha_t)}{\partial \alpha_t^2} \Big|_{\hat{a}_t}$, which is independent of \hat{p}_t . Thus, the approximation error remains of order \hat{p}_t^2 even when employing the negative Hessian in place of the squared score. We conclude that the method of Section (2.2), recovered by writing the recursions for linear-Gaussian models in terms of the score, can be derived as a first-order Taylor expansion in the neighbourhood of the optimal filter and satisfies the result in Prop. 3.

The constraint $p(y_t|Y_{t-1}) = p(y_t|\alpha_t)|_{\hat{a}_t}$ specifies, given the nonlinear non-Gaussian model in Eq. (2.3.1), (2.3.2), how the conditional density appearing in the recursions of Section (2.2) must be set to guarantee that the resulting filtering algorithm satisfies the result in Prop. 3. It is worth noting that such constraint follows from the same linear approximation made to compute the approximate filter. Indeed, the following result holds (see Appendix E):

Proposition 4. *Under the assumptions of Prop. 1, the conditional density $p(y_t|Y_{t-1})$ of the nonlinear non-Gaussian model in Eq. (2.3.1), (2.3.2) is given by:*

$$p(y_t|Y_{t-1}) = p(y_t|\alpha_t)|_{\hat{a}_t} + \mathcal{O}(\hat{p}_t) \quad (2.3.16)$$

It would be interesting to characterize the relation between the static parameters maximizing the true log-likelihood function $L = \sum_{t=1}^n \log p(y_t|Y_{t-1})$ and those recovered by maximizing the approximate log-likelihood function $\hat{L} = \sum_{t=1}^n \log p(y_t|\alpha_t)|_{\hat{a}_t}$. This is a highly nonlinear problem whose investigation is left for future work. For the models considered in the simulation study in Section (3), we found that the empirical density function of the maximum likelihood estimates of the parameters c, ϕ, q appearing in the transition equation is centred around the true values, whereas we found a bias for the parameters appearing in the observation density.

We finally point out that the above results can be extended into several directions. For instance, one can compute higher-order conditional moments to better characterize the conditional density of the state variables or consider an higher-order expansion of the observation density to improve the approximation.

2.4 Relation with observation-driven models

The predictive filter in Eq. (2.1.7) belongs to the class of score-driven models of Creal et al. (2013) and Harvey (2013). Specifically, in score-driven models, the vector of time-varying parameters \mathbf{a}_t evolves as:

$$\mathbf{a}_{t+1} = \mathbf{c} + \mathbf{T}\mathbf{a}_t + \mathbf{A}\mathbf{S}_t\nabla_t \quad (2.4.1)$$

where \mathbf{S}_t is an arbitrary normalization matrix that accounts for the curvature of the conditional log-likelihood. The update in Eq. (2.2.5) is obtained by setting $\mathbf{S}_t = \mathbf{A}^{-1}\mathbf{T}\mathbf{P}_t$ and letting \mathbf{P}_t evolve based on Eq. (2.2.7). Thus, the general representation in Eq. (2.2.5) picks up a particular normalization that is consistent with the update in the Kalman filter. Compared to the typical normalization adopted in score-driven models, based on inverse powers of the Fisher information, such normalization has two interesting features. First, in nonlinear non-Gaussian models, the Hessian generally depends on the observations, and so the normalization matrix itself does. This is natural, as it means that not only first, but even the second conditional moments are driven by past observations. Second, the static parameters appearing in Eq. (2.2.5), namely the system matrices \mathbf{T} and \mathbf{Q} , have an immediate interpretation, as they are the same as those appearing in the DGP described by Eq. (2.3.1), (2.3.2). This one-to-one correspondence between the static parameters in the DGP and those in the approximate filtering algorithm is lost under different normalizations.

When \mathbf{S}_t is set differently, the conditional covariance \mathbf{P}_t must be defined by analogy. Specifically, we observe that Eq. (2.2.5) and (2.4.1) are the same as far as $\mathbf{P}_t = \mathbf{T}^{-1}\mathbf{A}\mathbf{S}_t$. We can thus apply the approximate recursions for the first and second moments with the matrix \mathbf{P}_t given by the previous expression. The experiments performed in our simulation study suggest that the choice of the scaling matrix does not affect significantly the performance of the methodology when filtering nonlinear non-Gaussian models. However, the use of the particular normalization given by Eq. (2.2.7) is essential when dealing with models with a number of latent components larger than the number of signals, i.e. when $m > p$. In this case, defining the conditional covariance as $\mathbf{P}_t = \mathbf{T}^{-1}\mathbf{A}\mathbf{S}_t$ might not be enough to uniquely identifying² the matrix \mathbf{A} . We provide more details on this point in Appendix F.

2.5 Relation with other approximate filtering methods

Masreliez (1975) proposed a popular filtering algorithm based on the score of the conditional density. The approximation at the basis of his algorithm is fundamentally different from the linear approximation considered in this paper. Indeed, to derive the approximate filtering recursions, he

²We thank Andrew Harvey for pointing this out.

assumed that the posterior density $p(\boldsymbol{\alpha}_t|\mathbf{Y}_{t-1})$ is normal. Such assumption leads to a set of recursions depending on the score and the Hessian matrix. However, they are computed with respect to a different approximate conditional density. The latter is indeed given by:

$$\hat{p}(\mathbf{y}_t|\mathbf{Y}_{t-1}) = \int_{\mathbb{R}^m} p(\mathbf{y}_t|\boldsymbol{\alpha}_t)\hat{p}(\boldsymbol{\alpha}_t|\mathbf{Y}_{t-1})d\boldsymbol{\alpha}_t \quad (2.5.1)$$

where $\hat{p}(\mathbf{y}_t|\mathbf{Y}_{t-1})$ is the normal approximate posterior density. Thus, at each time-step, one needs to compute the convolution in Eq. (2.5.1), which differs from the simple approximate conditional density $p(\mathbf{y}_t|\boldsymbol{\alpha}_t)|_{\hat{\boldsymbol{\alpha}}_t}$ recovered in Section (2.3). Similarly, the expressions of the first and second derivatives are different from those recovered in our method. Furthermore, it is not clear how one can quantify the approximation error made by replacing the true posterior density $p(\boldsymbol{\alpha}_t|\mathbf{Y}_{t-1})$ with the approximate normal density $\hat{p}(\boldsymbol{\alpha}_t|\mathbf{Y}_{t-1})$.

The proposed method is also related to the class of approximating linear-Gaussian models proposed by Durbin and Koopman (1997) and Durbin and Koopman (2012) to set the parameters of the density used in the importance sampling method for nonlinear non-Gaussian models. These authors construct a sequence of linear Gaussian models that approximate the nonlinear non-Gaussian model in a neighbourhood of the conditional mode. The approximating linear-Gaussian model at the j -th iteration has the form of Eq. (2.1.1), (2.1.2), with \mathbf{y}_t replaced by:

$$\tilde{\mathbf{y}}_t^{(j)} = \mathbf{Z}\tilde{\boldsymbol{\alpha}}_t^{(j-1)} - \ddot{\mathbf{h}}_t^{(j-1)}\dot{\mathbf{h}}_t^{(j)} \quad (2.5.2)$$

where

$$\dot{\mathbf{h}}_t^{(j)} = -\frac{\partial \log p(\mathbf{y}_t|\boldsymbol{\alpha}_t)}{\partial \boldsymbol{\alpha}_t} \Big|_{\tilde{\boldsymbol{\alpha}}_t^{(j-1)}}, \quad \ddot{\mathbf{h}}_t^{(j)} = -\frac{\partial^2 \log p(\mathbf{y}_t|\boldsymbol{\alpha}_t)}{\partial \boldsymbol{\alpha}_t \partial \boldsymbol{\alpha}_t'} \Big|_{\tilde{\boldsymbol{\alpha}}_t^{(j-1)}} \quad (2.5.3)$$

and the matrix \mathbf{H} replaced by $\tilde{\mathbf{H}}_t^{(j)} = \ddot{\mathbf{h}}_t^{(j-1)}$ at each time-step. Here, $\tilde{\boldsymbol{\alpha}}_t^{(j-1)}$ denotes the smoothed estimate obtained from the previous iteration of the Kalman filter and smoother recursions and $p(\mathbf{y}_t|\boldsymbol{\alpha})$ is the observation density of the nonlinear non-Gaussian model. The method proceeds iteratively by running new Kalman filter and smoother recursions having $\tilde{\mathbf{H}}_t^{(j)}$ and $\tilde{\mathbf{y}}_t^{(j)}$ as an input. Shephard and Pitt (1997) recovered the same approximation although using a different approach.

Even in this method, the approximate recursions are driven by the score and the Hessian of the conditional density. However, the latter are evaluated at the trial value $\tilde{\boldsymbol{\alpha}}_t^{(j-1)}$ recovered from the previous run of the Kalman filter and smoother recursions. In the method described in Section (2.2), they are instead evaluated at $\hat{\boldsymbol{\alpha}}_t$, namely at the prediction recovered at the previous time-step. As such, contrary to our method, the mode approximation technique has not the form of standard observation-driven models. Rather, each run of the Kalman filter and smoother can be seen as an iteration of a Newton-Raphson method in the space spanned by the state-variables, as formally shown by Durbin and Koopman (2012).

2.6 Parameter and filtering uncertainty

As underlined by Blasques et al. (2016), confidence bands in observation-driven models can reflect parameter, filtering uncertainty or both. Parameter uncertainty arises when the true static parameters are replaced by their maximum-likelihood estimates. Confidence bands accounting for parameter uncertainty can be constructed using the methods developed e.g. by Pascual et al. (2006) and Blasques et al. (2016).

Filtering uncertainty becomes relevant when the time-varying parameters are not completely revealed by past observations. It is therefore absent in correctly specified observation-driven models, where the time-varying parameters are one-step-ahead predictable. In contrast, if observation-driven models are employed as misspecified filters, one is interested in constructing confidence bands reflecting the conditional density of the underlying state variables. The recursions in Eq. (2.2.5)-(2.2.7) provide the approximate second moments of the conditional density. To construct approximate confidence bands at a given confidence level, one can assume a normal conditional density. The Monte Carlo analysis in Section (3) shows that, for state-space models characterized by a nonlinear non-Gaussian observation density but linear transition equation, the normal approximation leads to a good matching between the nominal confidence level and the average coverage of the bands.

When score-driven models are employed as misspecified filter, it is essential to construct confidence bands reflecting both parameter and filtering uncertainty. Following Hamilton (1986), this can be done by adopting the Bayesian perspective that the vector of static parameters, that we denote by $\boldsymbol{\theta}$, is a random variable with a certain prior distribution $p(\boldsymbol{\theta})$. In practice, $p(\boldsymbol{\theta})$ can be set equal to the asymptotic distribution of the maximum likelihood estimate $\hat{\boldsymbol{\theta}}$, as in Blasques et al. (2016). Let $\mathbf{a}_t^{\hat{\boldsymbol{\theta}}}$ denote the predictive filter computed from $\hat{\boldsymbol{\theta}}$. It is possible to show (Hamilton 1986) that the total conditional variance can be decomposed into the sum of two terms:

$$\begin{aligned} & \mathbb{E}[(\boldsymbol{\alpha}_t - \mathbf{a}_t^{\hat{\boldsymbol{\theta}}})(\boldsymbol{\alpha}_t - \mathbf{a}_t^{\hat{\boldsymbol{\theta}}})' | \mathbf{Y}_{t-1}] = \\ & \mathbb{E}_{\boldsymbol{\theta}}[(\boldsymbol{\alpha}_t - \mathbf{a}_t^{\boldsymbol{\theta}})(\boldsymbol{\alpha}_t - \mathbf{a}_t^{\boldsymbol{\theta}})' | \mathbf{Y}_{t-1}] + \mathbb{E}_{\boldsymbol{\theta}}[(\mathbf{a}_t^{\boldsymbol{\theta}} - \mathbf{a}_t^{\hat{\boldsymbol{\theta}}})(\mathbf{a}_t^{\boldsymbol{\theta}} - \mathbf{a}_t^{\hat{\boldsymbol{\theta}}})'] = \\ & \mathbb{E}_{\boldsymbol{\theta}}[\mathbf{P}_t^{\boldsymbol{\theta}}] + \mathbb{E}_{\boldsymbol{\theta}}[(\mathbf{a}_t^{\boldsymbol{\theta}} - \mathbf{a}_t^{\hat{\boldsymbol{\theta}}})(\mathbf{a}_t^{\boldsymbol{\theta}} - \mathbf{a}_t^{\hat{\boldsymbol{\theta}}})'] \end{aligned} \quad (2.6.1)$$

where $\mathbb{E}_{\boldsymbol{\theta}}[\cdot]$ denotes the expectation taken with respect to the prior density $p(\boldsymbol{\theta})$. The first term is related to filtering uncertainty. It represents the conditional variance of the state variables averaged over the density $p(\boldsymbol{\theta})$. The second term is clearly related to parameter uncertainty, as it represents the variance of $\mathbf{a}_t^{\boldsymbol{\theta}}$ due to the randomness of $\boldsymbol{\theta}$ around the maximum likelihood estimate $\hat{\boldsymbol{\theta}}$. Both terms can be computed by simulations, sampling from the prior density $p(\boldsymbol{\theta})$ and then taking the sample mean.

3 Monte Carlo analysis

In this section we examine by Monte Carlo simulations the performance of the approximate algorithm of Section (2.2). We start by analysing the first conditional moments and afterwards we concentrate on the second conditional moments. As a data generating process, we consider several nonlinear non-Gaussian state-space models for location, scale and duration. To assess the loss of efficiency due to our approximation, we compare the filtered and smoothed estimates recovered by our methodology with those obtained from exact simulation-based methods. In particular, to estimate the static parameters, we use the “Numerically Accelerated Importance Sampling” (NAIS) method of Koopman et al. (2015), in a similar fashion to Koopman et al. (2016). Filtered and smoothed estimates are then computed by importance sampling, as described by Durbin and Koopman (2012).

The state-space models considered in this analysis have the form of Eq. (2.3.1), (2.3.2). In particular, we concentrate on the following models:

$$\begin{aligned}
 \text{Location (Student-}t\text{):} & \quad y_t = \alpha_t + \eta_t, \quad \eta_t \sim t_\nu(0, e^\lambda) \\
 \text{Scale (Gaussian):} & \quad y_t = e^{\omega + \alpha_t} \epsilon_t, \quad \epsilon_t \sim N(0, 1) \\
 \text{Scale (Student-}t\text{):} & \quad y_t = e^{\omega + \alpha_t} \epsilon_t, \quad \epsilon_t \sim t_\nu(0, 1) \\
 \text{Duration (Poisson):} & \quad y_t \sim \text{Poiss}(\alpha_t)
 \end{aligned}$$

The state variable α_t follows the process in Eq. (2.3.2), and for simplicity we set η_t being normal:

$$\alpha_{t+1} = c + \phi\alpha_t + \eta_t, \quad \eta_t \sim N(0, q)$$

The first model is linear in the location parameter, but has Student- t distributed measurement errors with scale e^λ . The second and third models are both nonlinear stochastic volatility models. They differ because of the observation density, which is Gaussian in the first model and Student- t in the second. The last is a stochastic duration model with a Poisson density. Such models have been applied extensively in the economic and finance literature. Few examples are given by Harvey et al. (1994), Ghysels et al. (1996) and Bauwens and Veredas (2004).

In order to run the filtering algorithm described in Section (2.2), we need to specify the conditional density $p(y_t|Y_{t-1})$ used to compute the score. The results of Section (2.3) guarantee that, if one sets $p(y_t|Y_{t-1}) = p(y_t|\alpha_t)|_{\hat{a}_t}$, the corresponding approximate filter obeys Prop. 3 and can therefore be regarded as resulting from a first-order expansion of $p(y_t|\alpha_t)$ around the optimal filter. We thus set $p(y_t|Y_{t-1}) = p(y_t|\alpha_t)|_{\hat{a}_t}$ throughout the analysis. Other choices of $p(y_t|Y_{t-1})$ are possible in principle. For instance, Koopman et al. (2016) choose a density with fatter tails in order to

better capture the over-dispersion generated by the true conditional density. However, there are no rigorous guidelines leading to the choice of the fatter tail density and the properties of the resulting filtering algorithm are unknown.

Model	Distribution	$p(y_t Y_{t-1})$	Normalization \mathbf{S}_t
Location	Student- t	$\frac{\Gamma(\frac{\nu+1}{2})}{\Gamma(\frac{\nu}{2})\sqrt{\pi(\nu-2)}e^\lambda} \log\left(1 + \frac{(y_t - a_t)^2}{(\nu-2)e^\lambda}\right)^{-\frac{\nu+1}{2}}$	$\frac{\nu}{\nu+1}e^{2\lambda}$
Scale	Gaussian	$\frac{1}{\sqrt{2\pi}e^{\omega+a_t}} \exp\left(-\frac{y_t^2}{2e^{\omega+a_t}}\right)$	1
Scale	Student- t	$\frac{\Gamma(\frac{\nu+1}{2})}{\Gamma(\frac{\nu}{2})\sqrt{\pi(\nu-2)}e^{\omega+a_t}} \log\left(1 + \frac{(y_t)^2}{(\nu-2)e^{\omega+a_t}}\right)^{-\frac{\nu+1}{2}}$	1
Duration	Poisson	$\frac{a_t^{y_t} e^{-a_t}}{y_t!}$	e^{-a_t}

Table 1: For each state-space model, we specify the conditional density and the normalization used in the filtering algorithm of Section (2.2).

The general representation in Section (2.2) picks up a particular normalization of the score. As underlined in Section (2.4), the choice of the normalization does not affect significantly the performance of the filtering algorithm. Nevertheless, the use of Eq. (2.2.7) is relevant when dealing with models characterized by a number of latent components larger than the number of signals (see Appendix F). This case is examined in the empirical application in Section (4), where we consider a stochastic volatility model with multiple volatility components. Since the models considered here only have one latent component, we use the common normalization adopted in score-driven models. In particular, the score is scaled by a certain power of the inverse of the information quantity, as in Creal et al. (2013) and Harvey (2013). As discussed in Section (2.4), in this case the matrix \mathbf{P}_t is defined by setting $\mathbf{P}_t = \mathbf{T}^{-1}\mathbf{A}\mathbf{S}_t$. Table (1) specifies both the conditional densities and the normalization used in the filtering algorithm, whereas Table (2) reports the values of the static parameters of the four state-space models. These values are similar to those used by Koopman et al. (2016). However, we point out that the relative performance of the methodology is independent of the particular choice of the static parameters.

The Monte Carlo study is based on 1000 replications of $n = 4000$ observations of the state-space models described above. Each sample is divided into two sub-samples of equal size. The first sub-sample is used to estimate the models, whereas the second is used to compute the mean-square-error (MSE) of the filtered and smoothed estimates. The NAIS is implemented with antithetic variables and the likelihood is computed based on $N = 400$ paths of the state variable sampled from the importance density. The observation-driven models are estimated by maximizing numerically the approximate log-likelihood $\hat{L} = \sum_{t=1}^n \log p(y_t|\alpha_t)|_{\hat{a}_t}$.

Model	c	ϕ	q	λ	ω	ν
Location (Student- t)	0.01	0.98	0.01	0.01	-	5
Scale (Gaussian)	0	0.98	0.01	-	0.1	-
Scale (Student- t)	0	0.98	0.01	-	0.1	5
Duration (Poisson)	0.001	0.98	0.01	-	-	-

Table 2: Values of the static parameters used to simulate the four state-space models used in the analysis.

Table (3) reports the MSE obtained from the importance sampling (IS) method and from the score-driven (SD) algorithm of Section (2.2). We show the loss of the two filters and of the smoother. As a further benchmark, we report the performance of the Kalman filter in the case of the location model, and that of the quasi-maximum likelihood method (QMLE) of Harvey et al. (1994) in the case of the two stochastic volatility models. The MSE of our approximate filtering algorithm remains very close to that of the exact method based on importance sampling. Specifically, the average relative loss of the score-driven algorithm is lower than 2.5%. Koopman et al. (2016) found a similar results comparing the performance of correctly specified parameter-driven models and score-driven models. In contrast, the Kalman filter and the QMLE method perform significantly worse. Figure (1) compares, in one particular simulation, the out-of-sample smoothed estimates obtained with importance sampling and the score-driven algorithm, confirming that the difference between the two is very small. Not surprisingly, the computational times are much lower for the score-driven algorithm. The ratio between the time required for estimating the static parameters and computing the filtered and smoothed estimates in the two methods range from 150 to 800.

Using the same Monte Carlo sample, we compute out-of-sample confidence bands around filtered and smoothed estimates by exploiting the result in Eq. (2.6.1). The latter allows us to compute the conditional variance of the latent component by taking into account both parameter and filtering uncertainty. We consider three nominal confidence levels, $\alpha = 0.90, 0.95, 0.99$ and compute the quantile of the posterior distribution by assuming a normal density. The prior density of the static parameters is approximated by a normal density with mean equal to the maximum likelihood estimates and variance given by the inverse of the Hessian. As a benchmark, we consider the simulation-based method of Blasques et al. (2016), which only takes into account parameter uncertainty. For this method, we only report the coverage of the predictive filter, as the time-varying parameters are assumed to be one-step-ahead predictable. The results are reported in Table (4), which shows the average coverage rates of the filtered and smoothed estimates. The algorithm based on score-driven recursions provides a good matching between the nominal confidence levels

		Location (Student- t)	Scale (Gaussian)	Scale (Student- t)	Duration (Poisson)
IS	Pred.	0.0986	0.1190	0.1342	0.0841
	Upd.	0.0921	0.1130	0.1287	0.0769
	Smooth.	0.0575	0.0790	0.0911	0.0471
SD	Pred.	0.0989	0.1215	0.1354	0.0860
	Upd.	0.0928	0.1156	0.1299	0.0787
	Smooth.	0.0576	0.0802	0.0921	0.0483
QMLE	Pred.	-	0.1613	0.1816	-
	Upd.	-	0.1569	0.1769	-
	Smooth	-	0.1126	0.1570	-
KF	Pred.	0.1059	-	-	-
	Upd.	0.0991	-	-	-
	Smooth.	0.0632	-	-	-

Table 3: We report the mean-square-error of the estimates of the four state-space models obtained through importance sampling (IS) and the score-driven (SD) algorithm of Section (2.2). In the case of the location model, we also show the loss obtained through the standard Kalman filter (KF), whereas in the case of the two stochastic volatility models we show the loss obtained through the QMLE method of Harvey et al. (1994)

and the average coverage rates. Such result is relevant especially in light of the performance of the method of Blasques et al. (2016), which, being based on parameter uncertainty only, underestimates significantly the total uncertainty. We thus conclude that accounting for filtering uncertainty is fundamental to accurately compute confidence bands in misspecified score-driven models.

4 Empirical application

In this section we provide empirical evidence that employing observation-driven models as misspecified filters offers a more accurate description of the dynamics of the time-varying parameters. In this perspective, volatility modelling represents an ideal framework, as we can assess the performance of the methodology by comparing the approximate first and second conditional moments with the realized measures constructed from high-frequency data (see e.g. Andersen and Bollerslev 1997, Andersen et al. 2003, Barndorff-Nielsen and Shephard 2004). However, we emphasize

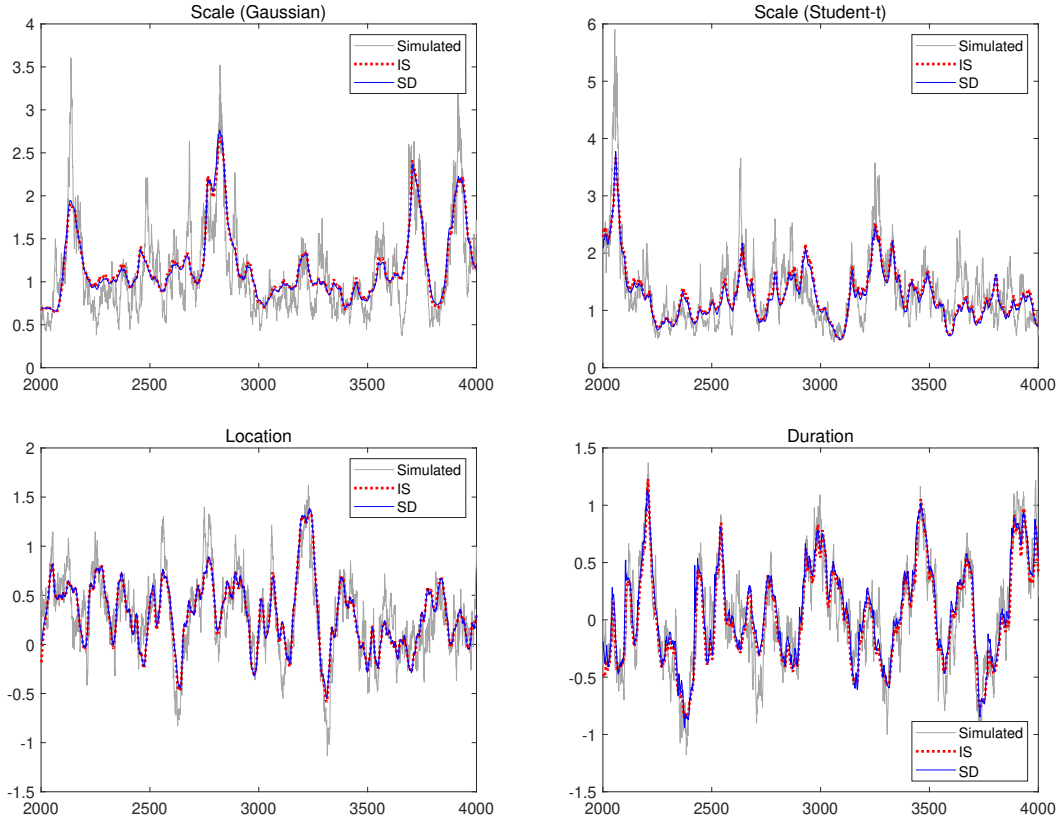


Figure 1: For one particular simulation, we show the out-of-sample smoothed estimates of the state-variable α_t recovered through importance sampling and the proposed score-driven algorithm. In the case of the two stochastic volatility models, we show the pattern of $e^{\omega+\alpha_t}$.

that the methodology remains formally unchanged in empirical problems characterized by different time-varying parameters and by different conditional distributions.

Let us consider the following two-component stochastic volatility model:

$$y_t = e^{\frac{\theta_t}{2}} \epsilon_t \quad (4.0.1)$$

$$\theta_t = \omega + \mathbf{Z}\alpha_t \quad (4.0.2)$$

$$\alpha_{t+1} = \mathbf{T}\alpha_t + \eta_t, \quad \eta_t \sim N(\mathbf{0}, \mathbf{Q}) \quad (4.0.3)$$

where $\epsilon_t \sim t_\nu$, $\mathbf{Z} = (1, 1)$, $\mathbf{T} = \text{diag}(\phi_1, \phi_2)$ and $\mathbf{Q} \in \mathbb{R}^{2 \times 2}$. Two-component volatility models have been advocated for instance by Engle and Lee (1999), Alizadeh et al. (2002) and Andersen et al. (2006) and are known to display long memory behaviour. The two volatility components can be interpreted as representing a slow factor responsible for the long-term dynamics of volatility and a fast factor responsible for the after-shocks following large volatility movements (see Harvey 2013 for a discussion).

We work with 1-minute transaction data of ExxonMobil (XOM) over the period from 01-12-

		Location (Student- t)	Scale (Gaussian)	Scale (Student- t)	Duration (Poisson)
		$\alpha = 0.90$			
Par. & Filt.	Pred.	0.8931	0.9018	0.8952	0.8849
	Upd.	0.8929	0.9016	0.8947	0.8834
	Smooth.	0.8976	0.9027	0.8956	0.8825
Par.	Pred.	0.8357	0.8363	0.8291	0.8321
		$\alpha = 0.95$			
Par. & Filt.	Pred.	0.9380	0.9473	0.9392	0.9386
	Upd.	0.9379	0.9473	0.9389	0.9378
	Smooth.	0.9421	0.9476	0.9383	0.9389
Par.	Pred.	0.8627	0.8541	0.8544	0.8761
		$\alpha = 0.99$			
Par. & Filt.	Pred.	0.9827	0.9871	0.9842	0.9796
	Upd.	0.9829	0.9871	0.9842	0.9800
	Smooth.	0.9856	0.9870	0.9842	0.9802
Par.	Pred.	0.9218	0.9067	0.8976	0.9433

Table 4: We report the average coverage rates of the out-of-sample confidence bands constructed around filtered and smoothed estimates at confidence levels $\alpha = 0.90, 0.95, 0.99$. For the predictive filter, we also report the average coverage rate obtained through the method of Blasques et al. (2016), which only accounts for parameter uncertainty.

1999 to 27-09-2013, including 3478 business days. For each day t , we construct (i) the daily return y_t computed as the difference between the closing and the opening log-prices and (ii) the realized variance RV_t obtained as the sum of squared 5-minutes returns. In light of the results of Andersen et al. (2003), RV_t is a consistent estimator of the so-called daily integrated variance. Thus, for the purpose of computing the mean-square errors and assessing the average coverage of the confidence bands, we use $\log RV_t$ as if it was the true latent log-variance θ_t .

To run the recursions in Section (2.2), we need to make a choice for the conditional density $p(y_t|Y_{t-1})$. Following the discussion in Section (2.3) and in Section (3), we set $p(y_t|Y_{t-1}) =$

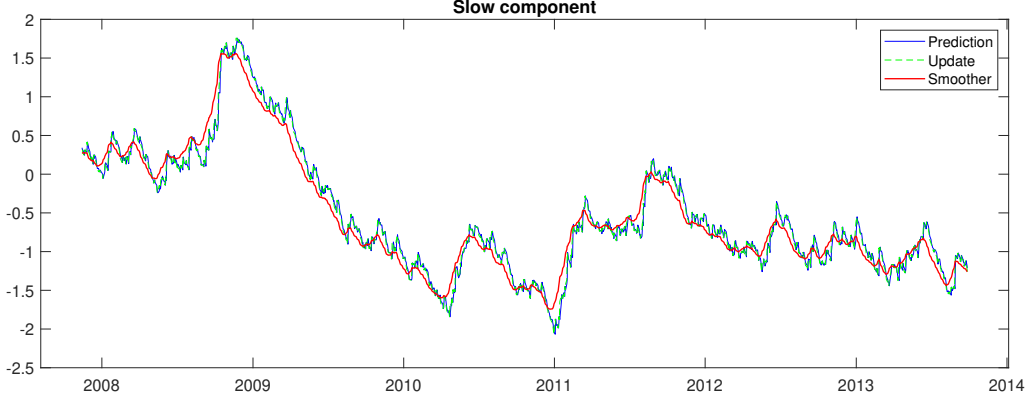


Figure 2: We show the out-of-sample filtered and smoothed estimates of the slow volatility component $\alpha_t^{(1)}$ of XOM.

$p(y_t|\theta_t)|_{\kappa_t}$, namely:

$$\begin{aligned} \log p(y_t|Y_{t-1}) &= \log \Gamma\left(\frac{\nu+1}{2}\right) - \log \Gamma\left(\frac{\nu}{2}\right) - \frac{1}{2} \log \pi - \frac{1}{2} \log(\nu-2) \\ &\quad - \frac{\kappa_t}{2} - \frac{\nu+1}{2} \log \left[1 + \frac{y_t^2}{(\nu-2)e^{\kappa_t}}\right] \end{aligned} \quad (4.0.4)$$

where $\kappa_t = \omega + \mathbf{Z}\mathbf{a}_t$ and \mathbf{a}_t is computed iteratively through Eq. (2.2.5), (2.2.7). Contrary to what we have done in the Monte Carlo study, we now set the score normalization as in Eq. (2.2.7). Such choice allows us to uniquely identify the conditional covariance \mathbf{P}_t and the smoother $\hat{\alpha}_t$, as discussed in Appendix F.

We estimate the parameters ν , ω , \mathbf{T} , \mathbf{Q} in the first sub-sample of $n = 2000$ business days. The out-of-sample filtered and smoothed estimates are then computed in the remaining sub-sample of 1478 days, from 14-11-2007 to 27-09-2013. In the following, we show the maximum likelihood estimates of the parameters:

$$\begin{aligned} \tilde{\omega} &= 0.0101, & \tilde{\phi}_1 &= 0.9992, & \tilde{\phi}_2 &= 0.9088, & \tilde{\nu} &= 9.7201 \\ \tilde{\mathbf{Q}}_{11} &= 0.0037, & \tilde{\mathbf{Q}}_{22} &= 0.0165, & \tilde{\mathbf{Q}}_{12} &= 0.0073 \end{aligned}$$

As commonly found in two-component models, the slow factor has large persistence ($\tilde{\phi}_1 \approx 1$) and lower variance ($\tilde{\mathbf{Q}}_{11} \ll \tilde{\mathbf{Q}}_{22}$). Fig. (2) and (3) show out-of-sample filtered and smoothed estimates of the two volatility factors, whereas Fig. (4) shows the out-of-sample log-variance obtained by summing the two factors and adding the intercept $\tilde{\omega}$.

To assess the extent to which the filtered and smoothed log-variances are good estimates of the

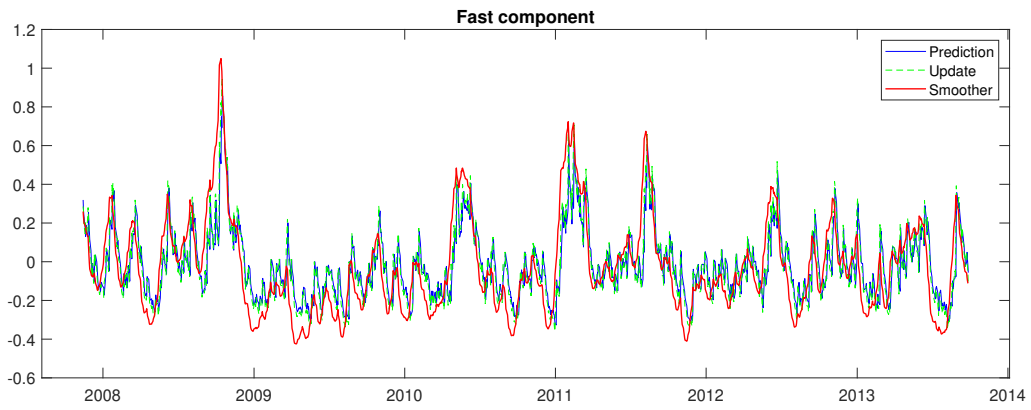


Figure 3: We show the out-of-sample filtered and smoothed estimates of the fast volatility component $\alpha_t^{(2)}$ of XOM.

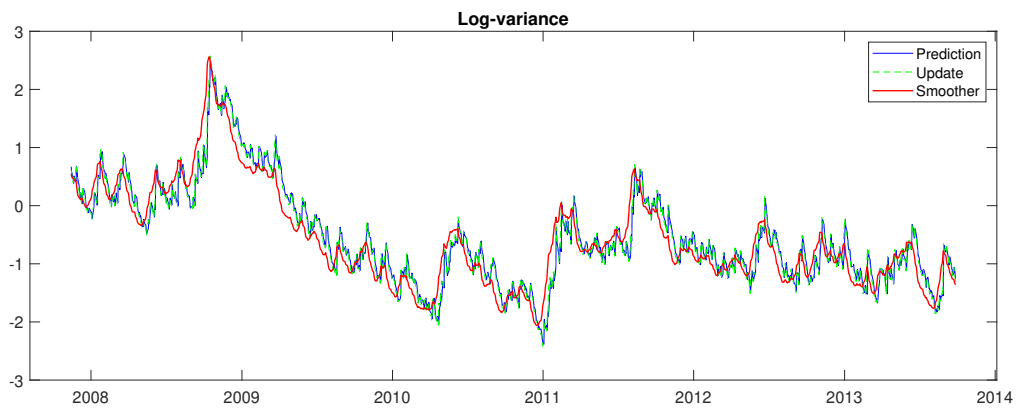


Figure 4: We show the out-of-sample filtered and smoothed estimates of the log-variance $\theta_t = \omega + \mathbf{Z}\alpha_t$ of XOM.

latent log-variance, we compute the following out-of-sample loss measures:

$$\begin{aligned}\text{MSE}^{(p)} &= \frac{1}{1478} \sum_{t=2001}^{3478} (\log RV_t - \kappa_t)^2 \\ \text{MSE}^{(u)} &= \frac{1}{1478} \sum_{t=2001}^{3478} (\log RV_t - \kappa_{t|t})^2 \\ \text{MSE}^{(s)} &= \frac{1}{1478} \sum_{t=2001}^{3478} (\log RV_t - \hat{\kappa}_t)^2\end{aligned}$$

where κ_t , $\kappa_{t|t}$ and $\hat{\kappa}_t$ denote the predictive filter, the update filter and the smoother, respectively. We find:

$$\text{MSE}^{(p)} = 0.3396, \quad \text{MSE}^{(u)} = 0.3021, \quad \text{MSE}^{(s)} = 0.2640^*$$

The star denotes the fact that $\text{MSE}^{(s)}$ is significantly lower than both $\text{MSE}^{(p)}$ and $\text{MSE}^{(u)}$, as resulting from the model confidence set test of Hansen et al. (2011) at 90% confidence level. Such empirical evidence suggests that volatility is not completely revealed by past observations, as correctly specified observation-driven models would suggest, and that exploiting the information coming from future returns helps to improve the estimation.

Correctly specified observation-driven models are only affected by parameter uncertainty. In light of the previous results, we expect that even filtering uncertainty plays a key role. To verify that this is true, we construct out-of-sample confidence bands as described in Section (2.6) and compare them with the confidence bands of Blasques et al. (2016), which only account for parameter uncertainty. Table (5) shows the average coverage of the confidence bands at different nominal confidence levels. As in the Monte Carlo study, we obtain that neglecting filtering uncertainty leads to underestimate the total uncertainty around the filtered estimates. To understand better this phenomenon, we plot in Fig. (5) the out-of-sample confidence bands obtained with the two methods, together with the logarithm of the 5-minutes realized variance. We clearly see that ignoring filtering uncertainty leads to narrow confidence bands and to a number of exceedances larger than what expected based on the choice of the nominal confidence level.

So far we have been focusing on a single stock. It is interesting to verify whether the recovered results hold for a multivariate time-series of stocks. To this end, we consider a dataset of 1-minute transaction data of Russel 3000 constituents covering the period from 18-11-1999 to 27-09-2013. The total number of assets is 4166. In order to avoid discontinuities due to changes in index composition, we concentrate on the sub-sample comprising the last 2000 business days. Assets having less than 10 trades per day are excluded in order to avoid poor and/or ill-conditioned realized covariance estimates. As a final outcome, we end up with 1682 assets.

		$\alpha = 0.90$	$\alpha = 0.95$	$\alpha = 0.99$
Par. & Filt.	Pred.	0.9039	0.9513	0.9817
	Upd.	0.9114	0.9520	0.9851
	Smooth.	0.8857	0.9381	0.9811
Par.	Pred.	0.6461	0.6922	0.7930

Table 5: For the asset XOM, we report the average coverage rates of the out-of-sample confidence bands constructed around filtered and smoothed estimates at confidence levels $\alpha = 0.90, 0.95, 0.99$. For the predictive filter, we also report the average coverage rate obtained through the method of Blasques et al. (2016), which only accounts for parameter uncertainty.

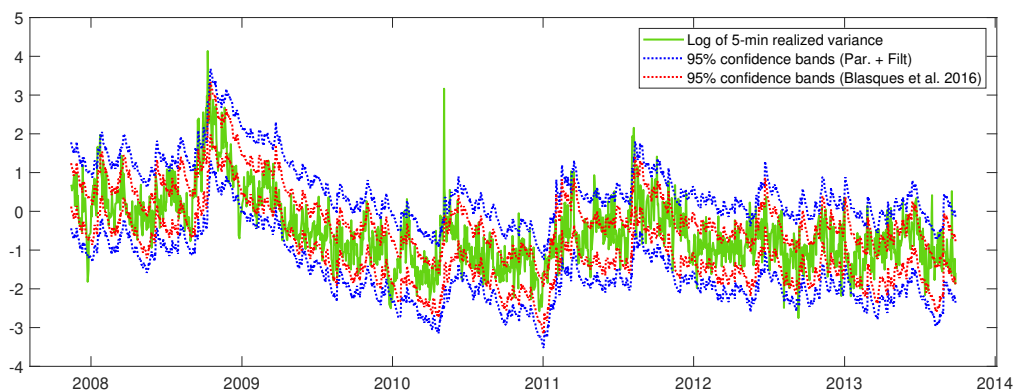


Figure 5: We show in green the logarithm of the 5-minute realized variance of XOM in the period from 14 Nov. 2007 to 27 Sep. 2013. We also report: the out-of-sample 95% confidence bands of the predicted filter computed by taking into account parameter and filtering uncertainty (blue) and the out-of-sample 95% confidence bands computed with the simulation-based method of Blasques et al. (2016) taking into account parameter uncertainty only (red).

Since we deal with multivariate time-series, we need a dynamic covariance model for vectors of log-returns. Specifically, we consider the t -GAS model of Creal et al. (2011), which is based on a multivariate Student- t conditional density. To guarantee positive-definite estimates, we implement the parameterization based on hyperspherical coordinates (see Creal et al. 2011). As the matrix \mathbf{A} multiplying the score is uniquely identifiable, we set the score normalization equal to the inverse of the Fisher information matrix. The number of time-varying parameters grows as p^2 , where p is the number of assets. As such, we can test the performance of our approximate filtering methodology in an highly multivariate framework where the use of exact simulation-based methods is computationally problematic or even infeasible.

Among the universe of $N = 1682$ assets, we randomly choose four portfolios of $p = 20$ assets.

	Portfolio 1	Portfolio 2	Portfolio 3	Portfolio 4
	MSE $\times 10^5$			
Pred.	0.7061	0.3705	0.2146	0.3255
Upd.	0.6950*	0.3634*	0.2099	0.3170*
Smooth.	0.6709*	0.3565*	0.1998*	0.3046*
	Qlike			
Pred.	-134.7951	-128.6277	-140.1625	-137.9562
Upd.	-135.1702	-129.0375	-140.5694	-138.2863
Smooth	-135.7584*	-129.3180*	-141.2055*	-138.8856*

Table 6: MSE and Qlike of filtered and smoothed estimates of the t -GAS model for the four randomly selected portfolios with $p = 20$. The star implies that the estimator is included in the model confidence set at 90% confidence level.

The loss measures used in this analysis are the MSE, computed as the Frobenius norm between matrices, and the Qlike (see Patton and Sheppard 2009). As a realized covariance estimator, we employ the estimator of Barndorff-Nielsen and Shephard (2004) computed on 5-minute log-returns. For each portfolio, the t -GAS is estimated on the first sub-sample of 1000 business days. We then compute, in the remaining sub-sample, the predictive filter, the update filter and the smoother. The statistical significance of loss differences is tested through the model confidence set at 90% confidence level.

Table (6) shows the results of the analysis. Even in this multivariate application, we obtain that the covariance estimates constructed through the predictive filter feature larger MSE and Qlike and are always excluded from the model confidence set. The covariance estimates built through the update filter and the smoother are both included in the model confidence set when considering the MSE as a loss measure. If the Qlike is considered instead, only smoothed estimates are included. Such results are similar to those found in the univariate application and confirm the relevance of employing observation-driven models as misspecified filters.

5 Conclusions

Correctly specified observation-driven models are purely predictive, meaning that past observations include all the relevant information related to the dynamics of the time-varying parameters. As such, there is no room for smoothing and the only form of uncertainty is that coming from replacing the true static parameters with their maximum-likelihood estimates.

In this paper we adopt a different view and assume that observation-driven models are misspecified filters, meaning that data are generated by a different dynamic specification, typically a nonlinear non-Gaussian state-space model. In this framework, the time-varying parameters are not completely revealed by past observations, and thus one needs a methodology for smoothing and for assessing filtering uncertainty.

Starting from a general representation of the Kalman filter and smoothing recursions in terms of the score of the conditional density, we recover a methodology for computing the first two conditional moments of the underlying state variables in misspecified score-driven models. This allows us to obtain, in addition to the predictive filter, the update filter, the smoother and to build in-sample and out-of-sample confidence bands accounting for both parameter and filtering uncertainty.

We prove that, given a nonlinear non-Gaussian state-space model, the proposed filtering algorithm results from a first-order Taylor expansion of the true observation density around the optimal filter. Such result allows us to quantify the approximation error and provides guidelines for the choice of the conditional density to employ in the approximate filtering and smoothing recursions.

In the simulation study, we find small differences in mean-square errors between our approximate method and importance sampling based techniques. However, it is worth highlighting that the exact methods are much more expensive from a computational point of view, requiring Monte Carlo integration and the choice of an importance density.

Filtering uncertainty plays a key role when computing confidence bands in misspecified score-driven models. We show in simulations that neglecting filtering uncertainty leads to narrow confidence bands and to a number of exceedances that is significantly larger than what expected from the choice of the nominal confidence level.

These results have relevant implications when applying observation-driven models to real data. If the latter are better described by a nonlinear non-Gaussian model, the use of correctly specified observation-driven models may be too restrictive, as one can not exploit the information of contemporaneous and future observations to estimate the time-varying parameters. Furthermore, it leads to narrow confidence bands, which may have deep policy and institutional implications. These findings are evidenced on empirical data using both univariate and multivariate stochastic volatility models, which are readily implementable in our methodology.

References

- Alizadeh, S., Brandt, M. W., Diebold, F. X., 2002. Range-based estimation of stochastic volatility models. *The Journal of Finance* 57 (3), 1047–1091.
- Andersen, T., Bollerslev, T., 1997. Intraday periodicity and volatility persistence in financial markets. *Journal of Empirical Finance* 4 (2-3), 115–158.
- Andersen, T. G., Bollerslev, T., Christoffersen, P. F., Diebold, F. X., 2006. Volatility and Correlation Forecasting. Vol. 1 of *Handbook of Economic Forecasting*. Elsevier, Ch. 15, pp. 777–878.
- Andersen, T. G., Bollerslev, T., Diebold, F. X., Labys, P., 2003. Modeling and forecasting realized volatility. *Econometrica* 71 (2), 579–625.
- Babii, A., Chen, X., Ghysels, E., 2019. Commercial and residential mortgage defaults: Spatial dependence with frailty. *Journal of Econometrics* 212 (1), 47 – 77.
- Barndorff-Nielsen, O. E., Shephard, N., 2004. Econometric analysis of realized covariation: High frequency based covariance, regression, and correlation in financial economics. *Econometrica* 72 (3), 885–925.
- Bauwens, L., Veredas, D., 2004. The stochastic conditional duration model: A latent variable model for the analysis of financial durations. *Journal of Econometrics* 119 (2), 381 – 412.
- Blasques, F., Koopman, S. J., Lucas, A., 2015. Information-theoretic optimality of observation-driven time series models for continuous responses. *Biometrika* 102 (2), 325.
- Blasques, F., Koopman, S. J., Lasak, K., Lucas, A., 2016. In-sample confidence bands and out-of-sample forecast bands for time-varying parameters in observation-driven models. *International Journal of Forecasting* 32 (3), 875 – 887.
- Bollerslev, T., April 1986. Generalized autoregressive conditional heteroskedasticity. *Journal of Econometrics* 31 (3), 307–327.
- Caivano, M., Harvey, A., Luati, A., Mar 2016. Robust time series models with trend and seasonal components. *SERIEs* 7 (1), 99–120.
- Cox, D., 1981. Statistical analysis of time series: Some recent developments [with discussion and reply]. *Scandinavian Journal of Statistics* 8 (2), 93–115.
- Creal, D., Koopman, S. J., Lucas, A., 2011. A dynamic multivariate heavy-tailed model for time-varying volatilities and correlations. *Journal of Business & Economic Statistics* 29 (4), 552–563.

- Creal, D., Koopman, S. J., Lucas, A., 2013. Generalized autoregressive score models with applications. *Journal of Applied Econometrics* 28 (5), 777–795.
- Durbin, J., Koopman, S., 2012. *Time Series Analysis by State Space Methods: Second Edition*. Oxford Statistical Science Series. OUP Oxford.
- Durbin, J., Koopman, S. J., 1997. Monte Carlo maximum likelihood estimation for non-Gaussian state space models. *Biometrika* 84 (3), 669–684.
- Engle, R., 1982. Autoregressive conditional heteroscedasticity with estimates of the variance of United Kingdom inflation. *Econometrica* 50 (4), 987–1007.
- Engle, R. F., Lee, G. G. J., 1999. A long-run and short-run component model of stock return volatility. *Cointegration, Causality and Forecasting: A Festschrift in Honour of Clive W. J. Granger*. Oxford University Press.
- Ghysels, E., Harvey, A., Renault, E., 1996. Stochastic volatility. *Handbook of Statistics* 14.
- Hamilton, J. D., 1986. A standard error for the estimated state vector of a state-space model. *Journal of Econometrics* 33 (3), 387 – 397.
- Hansen, P. R., Lunde, A., Nason, J. M., 2011. The model confidence set. *Econometrica* 79 (2), 453–497.
- Harvey, A., 1991. *Forecasting, Structural Time Series Models and the Kalman Filter*. Cambridge University Press.
- Harvey, A., Luati, A., 2014. Filtering with heavy tails. *Journal of the American Statistical Association* 109 (507), 1112–1122.
- Harvey, A., Ruiz, E., Shephard, N., 1994. Multivariate stochastic variance models. *The Review of Economic Studies* 61 (2), 247–264.
- Harvey, A. C., 2013. *Dynamic Models for Volatility and Heavy Tails: With Applications to Financial and Economic Time Series*. Econometric Society Monographs. Cambridge University Press.
- Koopman, S. J., Lucas, A., Scharth, M., 2015. Numerically accelerated importance sampling for nonlinear non-Gaussian state-space models. *Journal of Business & Economic Statistics* 33 (1), 114–127.

- Koopman, S. J., Lucas, A., Scharth, M., March 2016. Predicting time-varying parameters with parameter-driven and observation-driven models. *The Review of Economics and Statistics* 98 (1), 97–110.
- Masreliez, C. J., 1975. Approximate non-Gaussian filtering with linear state and observation relations. *IEEE Transactions on Automatic Control* AC-20, 777–795.
- Nelson, D. B., 1992. Filtering and forecasting with misspecified ARCH models I: Getting the right variance with the wrong model. *Journal of Econometrics* 52 (1), 61 – 90.
- Nelson, D. B., 1996. Asymptotically optimal smoothing with ARCH models. *Econometrica* 64 (3), 561–573.
- Nelson, D. B., Foster, D. P., 1994. Asymptotic filtering theory for univariate ARCH models. *Econometrica* 62 (1), 1–41.
- Nelson, D. B., Foster, D. P., 1995. Filtering and forecasting with misspecified ARCH models II: Making the right forecast with the wrong model. *Journal of Econometrics* 67 (2), 303 – 335.
- Oh, D. H., Patton, A. J., 2017. Time-varying systemic risk: Evidence from a dynamic copula model of cds spreads. *Journal of Business & Economic Statistics* 0 (0), 1–15.
- Pascual, L., Romo, J., Ruiz, E., 2006. Bootstrap prediction for returns and volatilities in GARCH models. *Computational Statistics & Data Analysis* 50 (9), 2293 – 2312.
- Patton, A. J., Sheppard, K., 2009. *Evaluating Volatility and Correlation Forecasts*. Springer Berlin Heidelberg, Berlin, Heidelberg, pp. 801–838.
- Shephard, N., Pitt, M. K., 1997. Likelihood analysis of non-Gaussian measurement time series. *Biometrika* 84 (3), 653–667.

Appendix

A Proof of Proposition 1

We first observe that, thanks to the Bayes rule, we can write:

$$p(\alpha_t|Y_t) = \frac{p(y_t|\alpha_t)p(\alpha_t|Y_{t-1})}{p(y_t|Y_{t-1})} \quad (\text{A.1})$$

Thus, the update filter $a_{t|t}$ can be written as:

$$a_{t|t} = \mathbb{E}[\alpha_t|Y_t] = \int_{\mathbb{R}} \alpha_t p(\alpha_t|Y_t) d\alpha_t = \int_{\mathbb{R}} \alpha_t \frac{p(y_t|\alpha_t)p(\alpha_t|Y_{t-1})}{p(y_t|Y_{t-1})} d\alpha_t \quad (\text{A.2})$$

Now, we consider the first-order Taylor expansion of $p(y_t|\alpha_t)$ around a_t . Thanks to the assumption that $p(y_t|\alpha_t) \in C^2(\mathbb{R})$, we have:

$$p(y_t|\alpha_t) = p(y_t|\alpha_t)|_{a_t} + \left. \frac{\partial p(y_t|\alpha_t)}{\partial \alpha_t} \right|_{a_t} (\alpha_t - a_t) + \mathcal{O}(\alpha_t - a_t)^2 \quad (\text{A.3})$$

Define:

$$p_*^{[1]}(y_t|\alpha_t) = p(y_t|\alpha_t)|_{a_t} + \left. \frac{\partial p(y_t|\alpha_t)}{\partial \alpha_t} \right|_{a_t} (\alpha_t - a_t) \quad (\text{A.4})$$

We require that the approximate update density $\frac{p_*^{[1]}(y_t|\alpha_t)p(\alpha_t|Y_{t-1})}{p(y_t|Y_{t-1})}$ integrates to one. Since:

$$\int_{\mathbb{R}} \frac{p_*^{[1]}(y_t|\alpha_t)p(\alpha_t|Y_{t-1})}{p(y_t|Y_{t-1})} d\alpha_t = \frac{p(y_t|\alpha_t)|_{a_t}}{p(y_t|Y_{t-1})} \quad (\text{A.5})$$

we re-define $p_*^{[1]}(y_t|\alpha_t)$ as:

$$p^{[1]}(y_t|\alpha_t) = p_*^{[1]}(y_t|\alpha_t) \frac{p(y_t|Y_{t-1})}{p(y_t|\alpha_t)|_{a_t}} = p(y_t|Y_{t-1}) \left[1 + \left. \frac{\partial \log p(y_t|\alpha_t)}{\partial \alpha_t} \right|_{a_t} (\alpha_t - a_t) \right] \quad (\text{A.6})$$

Therefore:

$$a_{t|t} = \int_{\mathbb{R}} \alpha_t \left[1 + \left. \frac{\partial \log p(y_t|\alpha_t)}{\partial \alpha_t} \right|_{a_t} (\alpha_t - a_t) + \mathcal{O}(\alpha_t - a_t)^2 \right] p(\alpha_t|Y_{t-1}) d\alpha_t \quad (\text{A.7})$$

Adding and subtracting a_t from the first factor and carrying out the integral, we obtain:

$$a_{t|t} = a_t + p_t \nabla_{t,a_t} + \mathcal{O}(p_t) \quad (\text{A.8})$$

whence the thesis. The computation of a_{t+1} is immediate:

$$a_{t+1} = \mathbb{E}[c + \phi \alpha_t + \eta_t | Y_t] = c + \phi a_{t|t} = c + \phi a_t + \phi p_t \nabla_{t,a_t} + \mathcal{O}(p_t) \quad (\text{A.9})$$

B Proof of Proposition 2

We have:

$$p_{t|t} = \mathbb{E}[(\alpha_t - a_{t|t})^2 | Y_t] = \mathbb{E}[(\alpha_t - a_t)^2 | Y_t] - (a_t - a_{t|t})^2 \quad (\text{B.1})$$

Using Prop. 1 and Corollary C, the second term is given by:

$$(a_t - a_{t|t})^2 = p_t^2 \nabla_{t,a_t}^2 + \mathcal{O}(p_t^2) \quad (\text{B.2})$$

We now compute the first term:

$$\mathbb{E}[(\alpha_t - a_t)^2 | Y_t] = \int_{\mathbb{R}} (\alpha_t - a_t)^2 \left[1 + \frac{\partial \log p(y_t | \alpha_t)}{\partial \alpha_t} \Big|_{\alpha_t} (\alpha_t - a_t) + \mathcal{O}(\alpha_t - a_t)^2 \right] p(\alpha_t | Y_{t-1}) d\alpha_t \quad (\text{B.3})$$

Using the assumption that $p(\alpha_t | Y_{t-1})$ is even and the fact that $\mathcal{O}(\mathbb{E}[(\alpha_t - a_t)^4]) = \mathcal{O}(\mathbb{E}[(\alpha_t - a_t)^2]^2)$, we have:

$$\mathbb{E}[(\alpha_t - a_t)^2 | Y_t] = p_t + \mathcal{O}(p_t^2) \quad (\text{B.4})$$

We conclude:

$$p_{t|t} = p_t(1 - p_t \nabla_t^2) + \mathcal{O}(p_t^2) \quad (\text{B.5})$$

The computation of p_{t+1} follows immediately:

$$p_{t+1} = \mathbb{V}[c + \phi \alpha_t + \eta_t | Y_t] = \phi^2 p_t(1 - p_t \nabla_t^2) + q + \mathcal{O}(p_t^2) \quad (\text{B.6})$$

C Proof of Corollary 1

The computation of a_{t+1} and p_{t+1} is carried out in Section A and B, respectively.

D Proof of Proposition 3

We need the following lemma:

Lemma 1. *Assume that the assumptions of Prop. 3 hold and that $a_t - \hat{a}_t = \mathcal{O}(p_t)$. Then:*

$$\nabla_{t,a_t} - \nabla_{t,\hat{a}_t} = \mathcal{O}(p_t) \quad (\text{D.1})$$

Proof.

Define:

$$f(\alpha) = \frac{\partial \log p(y_t | \alpha)}{\partial \alpha} \quad (\text{D.2})$$

As $p(y_t|\alpha) \in C^3(\mathbb{R})$, we can write:

$$f(\alpha) = \frac{\partial \log p(y_t|\alpha)}{\partial \alpha} \Big|_{a_t} + \frac{\partial^2 \log p(y_t|\alpha)}{\partial \alpha^2} \Big|_{a_t} (\alpha - a_t) + \mathcal{O}(\alpha - a_t)^2 \quad (\text{D.3})$$

and

$$f(\alpha) = \frac{\partial \log p(y_t|\alpha)}{\partial \alpha} \Big|_{\hat{a}_t} + \frac{\partial^2 \log p(y_t|\alpha)}{\partial \alpha^2} \Big|_{\hat{a}_t} (\alpha - \hat{a}_t) + \mathcal{O}(\alpha - \hat{a}_t)^2 \quad (\text{D.4})$$

where in the first line we expand $f(\alpha)$ around a_t , whereas in the second line we expand $f(\alpha)$ around \hat{a}_t . Evaluating both equations at $\alpha = a_t$ and then subtracting, we end up with:

$$\nabla_{t,a_t} - \nabla_{t,\hat{a}_t} - \frac{\partial^2 \log p(y_t|\alpha)}{\partial \alpha^2} \Big|_{\hat{a}_t} (a_t - \hat{a}_t) = 0 \quad (\text{D.5})$$

and therefore:

$$\nabla_{t,a_t} - \nabla_{t,\hat{a}_t} = \mathcal{O}(p_t) \quad (\text{D.6})$$

■

We prove Prop. 3 by induction. The case $t = 1$ is straightforward. We have:

$$\begin{aligned} a_{1|1} &= a_1 + \nabla_{1,a_1} p_1 + \mathcal{O}(p_1) \\ \hat{a}_{1|1} &= \hat{a}_1 + \nabla_{1,\hat{a}_1} \hat{p}_1 \end{aligned}$$

As $\hat{a}_1 = a_1$ and $\hat{p}_1 = p_1$ by assumption, we have:

$$a_{1|1} = \hat{a}_{1|1} + \mathcal{O}(\hat{p}_1) \quad (\text{D.7})$$

Similarly, it follows:

$$a_2 = \hat{a}_2 + \mathcal{O}(\hat{p}_1) \quad (\text{D.8})$$

For the variances we have:

$$p_{1|1} = p_1(1 - p_1 \nabla_{1,a_1}^2) + \mathcal{O}(p_1^2) \quad (\text{D.9})$$

$$\hat{p}_{1|1} = \hat{p}_1(1 - \hat{p}_1 \nabla_{1,\hat{a}_1}^2) \quad (\text{D.10})$$

thus:

$$p_{1|1} = \hat{p}_{1|1} + \mathcal{O}(\hat{p}_1^2) \quad (\text{D.11})$$

and similarly:

$$p_2 - \hat{p}_2 = \mathcal{O}(\hat{p}_1^2) \quad (\text{D.12})$$

Now, assume that Prop. 3 holds for $t-1$ and let us prove that it also holds for t . First, we compute

$a_{t|t} - \hat{a}_{t|t}$:

$$a_{t|t} - \hat{a}_{t|t} = (a_t - \hat{a}_t) + (\nabla_{t,a_t} p_t - \nabla_{t,\hat{a}_t} \hat{p}_t) + \mathcal{O}(p_t) \quad (\text{D.13})$$

The first term in parenthesis is $\mathcal{O}(\hat{p}_t)$ thanks to the inductive hypothesis and Eq. (2.3.10), whereas the second term is $\mathcal{O}(\hat{p}_t^2)$ by virtue of Lemma 1. Thus:

$$a_{t|t} = \hat{a}_{t|t} + \mathcal{O}(\hat{p}_t) \quad (\text{D.14})$$

For the variances we proceed analogously:

$$p_{t|t} - \hat{p}_{t|t} = (p_t - \hat{p}_t) - (p_t^2 \nabla_{t,a_t}^2 - \hat{p}_t^2 \nabla_{t,\hat{a}_t}^2) + \mathcal{O}(p_t^2) \quad (\text{D.15})$$

The first term in parenthesis is $\mathcal{O}(\hat{p}_t^2)$ thanks to the inductive hypothesis and Eq. (2.3.11), whereas the second contains higher order terms by virtue of Lemma 1. Thus:

$$p_{t|t} = \hat{p}_{t|t} + \mathcal{O}(\hat{p}_t^2) \quad (\text{D.16})$$

It is now immediate proving that analogous relations hold for a_{t+1} and p_{t+1} .

E Proof of Proposition 4

We have:

$$p(y_t|Y_{t-1}) = \int_{\mathbb{R}} p(y_t|\alpha_t)p(\alpha_t|Y_{t-1})d\alpha_t \quad (\text{E.1})$$

Using the Taylor expansion of $p(y_t|\alpha_t)$ in Eq. (A.3), we can write, up to a constant of normalization:

$$p(y_t|Y_{t-1}) = \int_{\mathbb{R}} \left[p(y_t|\alpha_t)|_{a_t} + \frac{\partial p(y_t|\alpha_t)}{\partial \alpha_t} \Big|_{a_t} (\alpha_t - a_t) + \mathcal{O}(\alpha_t - a_t)^2 \right] p(\alpha_t|Y_{t-1})d\alpha_t \quad (\text{E.2})$$

which gives:

$$p(y_t|Y_{t-1}) = p(y_t|\alpha_t)|_{a_t} + \mathcal{O}(p_t) \quad (\text{E.3})$$

The thesis follows by applying Prop. 3.

F The case with a scalar signal ($p = 1$) and more latent components ($m > 1$)

Let $y_t \in \mathbb{R}$, $\mathbf{a}_t \in \mathbb{R}^m$, $m > 1$ and $\mathbf{Z} \in \mathbb{R}^{1 \times m}$. Let us consider an observation density $p(y_t|\theta_t)$, where $\theta_t = \mathbf{Z}\mathbf{a}_t$ is a scalar signal. The score is given by:

$$\nabla_t = \frac{\partial \log p(y_t|\theta_t)}{\partial \mathbf{a}_t} = \mathbf{Z}' \nabla_t^{(\theta_t)} \quad (\text{F.1})$$

where $\nabla_t^{(\theta_t)} = \frac{\partial \log p(y_t|\theta_t)}{\partial \theta_t}$ is scalar. Similarly, the Fisher information matrix is given by:

$$\mathbf{I}_t = \mathbb{E}_{t-1}[\nabla_t \nabla_t'] = \mathbf{Z}' \mathbf{Z} i_t^{(\theta_t)} \quad (\text{F.2})$$

where $i_t^{(\theta_t)} = \mathbb{E}_{t-1}[\nabla_t^{(\theta_t)^2}]$ is scalar.

Let us consider the case in which \mathbf{a}_t evolves based on the score-driven scheme in Eq. (2.4.1):

$$\mathbf{a}_{t+1} = \mathbf{c} + \mathbf{T}\mathbf{a}_t + \mathbf{A}\nabla_t \tag{F.3}$$

where, since \mathbf{I}_t is singular, we have set $\mathbf{S}_t = \mathbb{I}$. Such choice for the normalization is equivalent to imposing a steady-state solution for the model. The last term can be written as $\mathbf{a}\nabla_t^{(\theta_t)}$, where $\mathbf{a} = \mathbf{A}\mathbf{Z}'$. It follows that we can only identify the vector \mathbf{a} , but not the full matrix \mathbf{A} . Similarly, since $\mathbf{P}_t = \mathbf{T}^{-1}\mathbf{A}$, we can only identify the vector $\mathbf{P}_t\mathbf{Z}'$, but not the full matrix \mathbf{P}_t . This is not an issue when computing the two filters in Eq. (2.2.4), (2.2.5), as they only depend on $\mathbf{P}_t\mathbf{Z}'$. In contrast, the smoother in Eq. (2.2.8), (2.2.9) depend on \mathbf{P}_t and thus we obtain different smoothed estimates depending on the choice of \mathbf{A} from the admissible set. The same argument can be generalized to the case $p > 1$ and $m > p$. In such cases, the matrix \mathbf{P}_t is identifiable provided that one uses the normalization given by Eq. (2.2.7), which is analogous to that used in the standard Kalman filter.